Turbulence of Second Sound Waves in Superfluid ^{4}He

Energy cascades & rogue waves in the laboratory

P.V.E. McClintock[1] V.B. Efimov[1,2] A.N. Ganshin[1]
G.V. Kolmakov[1,2] L.P. Mezhov-Deglin[2]

[1]Department of Physics, Lancaster University, UK

[2]Institute of Solid State Physics RAS, Chernogolovka, Russia

“Let’s Face Chaos”, Maribor, 7 July 2008

Outline

Outline

1. Introduction
   - Motivation
2. Modelling wave turbulence
   - Need for models
   - Second sound in He II
3. Experiments & results
   - Experimental set-up
   - Energy cascades
   - Transients & dynamics
4. Discussion
   - Wider implications
   - Conclusion

Cascades of energy through different length scales.

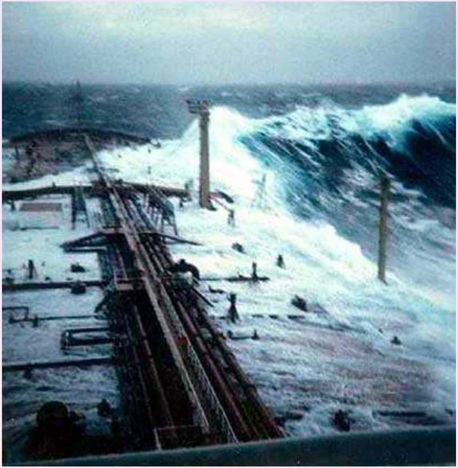

Outline

Turbulence in many forms

In addition to familiar vortex turbulence in fluids, turbulence can also occur in systems of waves, e.g. –

- Magnetic turbulence in interstellar gases.
- Shock waves in the solar wind.
- Sound waves in oceanic waveguides.
- Capillary waves on ocean surface.
- Phonon turbulence in solids.
- Second sound in He II...

Wave turbulence

Wave turbulence arises in systems of strongly interacting nonlinear waves.

It is similar to vortex turbulence in fluids in that –

- There is a flow of energy across the length scales – conventionally, from the scale of the driving towards smaller and smaller scales.
- At small enough scales dissipation (due to e.g. viscosity) becomes important and terminates the cascade.

It is believed that rogue waves on the ocean arise through nonlinear wave interactions...

Outline

Need for models

- In practice, it is difficult to test the theory of wave turbulence through studies of natural events (e.g. on ocean, in interstellar media).
- So a laboratory test-bed is needed, where parameters can be controlled and adjusted.
- It turns out that the properties of He II make it an ideal model system.

Outline

Sound modes in He II

Two sound modes in bulk He II –

- First sound is a pressure-density wave, with in-phase motion of the normal and superfluid components, and phase velocity

$$u_1 = \sqrt{\left(\frac{\partial P}{\partial \rho}\right)_\sigma}$$

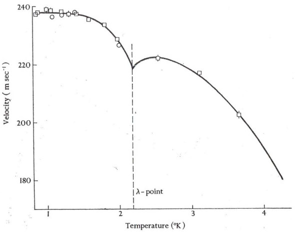

Sound modes in He II

Two sound modes in bulk He II –

- First sound is a pressure-density wave, with in-phase motion of the normal and superfluid components, and phase velocity

$$u_1 = \sqrt{\left(\frac{\partial P}{\partial \rho}\right)_\sigma}$$

- Second sound is an entropy-temperature wave, with anti-phase motion of the two components, and phase velocity

$$u_2 = \sqrt{\frac{\rho_s \sigma^2}{\rho_n}\left(\frac{\partial T}{\partial \sigma}\right)_\rho}$$

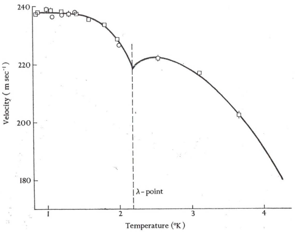

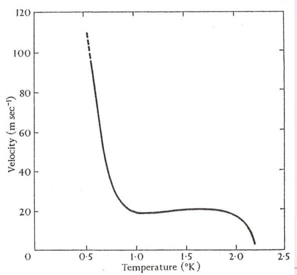

Nonlinear coefficient for second sound

- For finite temperature excursions δT, 2nd sound velocity is –

$$u_2 = u_{20}(1 + \alpha\delta T)$$

where the nonlinear coefficient

$$\alpha = \frac{\partial}{\partial T} \ln\left(u_{20}^3 \frac{C}{T}\right)$$

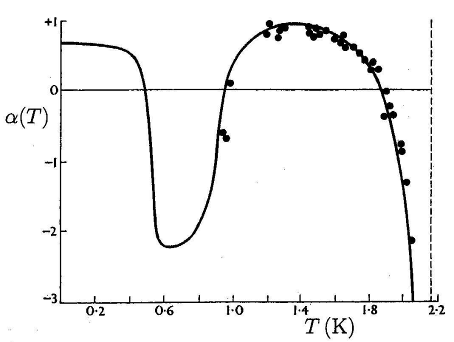

Datapoints: experiments, Dessler & Fairbank (1956).
Curve: theory, I M Khalatnikov (1952)

Nonlinear coefficient for second sound

- For finite temperature excursions δT, 2nd sound velocity is –

$$u_2 = u_{20}(1 + \alpha \delta T)$$

where the nonlinear coefficient

$$\alpha = \frac{\partial}{\partial T} \ln \left(u_{20}^3 \frac{C}{T} \right)$$

- Note –
  - $\alpha \rightarrow -\infty$ as $T \rightarrow T_\lambda$
  - α changes sign at $T = 1.88$ K

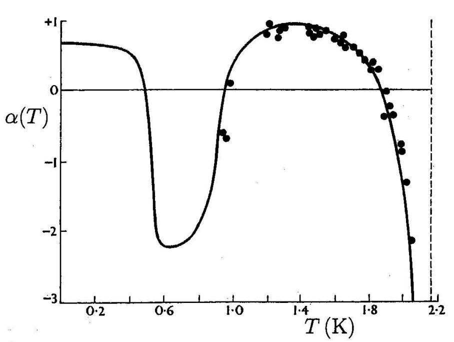

Datapoints: experiments, Dessler & Fairbank (1956).
Curve: theory, I M Khalatnikov (1952)

Advantages of second sound for modelling

So second sound offers many advantages as a model system for studying wave turbulence –

- Nonlinear coefficient α can be made very large.
- Also, α can be "tuned" by adjustment of T to be either
  - Positive, or
  - Negative, or
  - Zero.
- The small velocity ($20\ \mathrm{m\,s^{-1}}$) gives good time resolution and convenient experimental dimensions.
- It is easy to apply a variety of different signals to control the second sound generator.

Outline

Sketch of experimental arrangement

- Create 2nd sound standing wave with heater.
- Detect it with a bolometer.
- Sinewave of ω on heater
  $\Rightarrow$ 2nd sound at 2ω in He II.
- But any waveform can be applied.

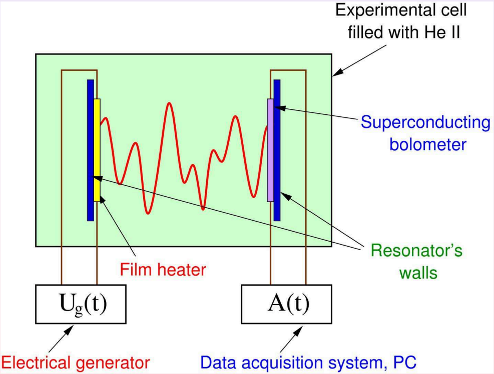

Construction of cell

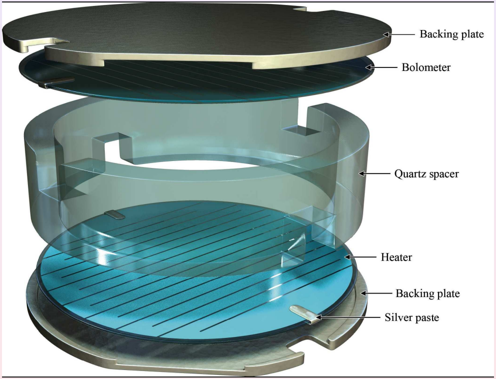

Aspect ratio of actual cell was different –

- Length of quartz spacer – 70 mm
- Inner diameter – 15 mm
- Endplates parallel to better that 1:10^4
- Thin film heater
- Thin film Sn-Cu bolometer
- Bolometer sensitivity – 2.6 $\mathrm{V\,K^{-1}}$
- $Q \sim 1000 - 3000$

Data recording

Experimental procedure –

- Drive heater from sinewave generator (0.1–100 kHz).
- Second sound wave amplitude $\delta T \sim$ 0.05–5.0 mK.
- Corresponding Mach number

  $\mathrm{M} = \alpha \delta T \sim 10^{-4} - 10^{-2}$.
- And acoustic Reynolds number

$$\mathrm{Re} = \frac{\alpha u_{20} \left(\partial \delta T / \partial x \right)}{\gamma_\omega} \sim \alpha Q \delta T$$

  can be adjusted in range ∼1–100.
- Record time series from bolometer (up to 10^6 points) and use FFT to compute power spectrum.

Outline

1. Introduction
   - Motivation
2. Modelling wave turbulence
   - Need for models
   - Second sound in He II
3. Experiments & results
   - Experimental set-up
   - Energy cascades
   - Transients & dynamics
4. Discussion
   - Wider implications
   - Conclusion

Power spectra of 2nd sound standing waves

- Driving on 31st resonance, $f_d = 3130\,\text{Hz}$.
- Heat flux W was –
  - (a) $5.5\ \text{mW cm}^{-2}$
  - (b) $22\ \ \text{mW cm}^{-2}$
- Dashed-line in (b) is $A_f \propto f^{3/2}$.
- Inset: amplitude at driving frequency v. heat flux.
- Arrows show viscous cut-off frequency.
- Kolmogorov-like direct energy cascade in (b).

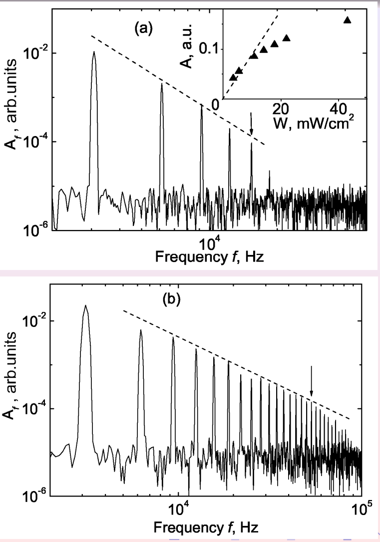

Numerical theory

- Calculations for 4 different driving force amplitudes F_d –
  - △ 0.01
  - ◇ 0.05
  - ○ 0.1
  - □ 0.3
- Dashed line is $A_f \propto f^{-1}$.
- Inset: standing wave amplitude at driving frequency for linear (dashed) and nonlinear (full curve) waves.

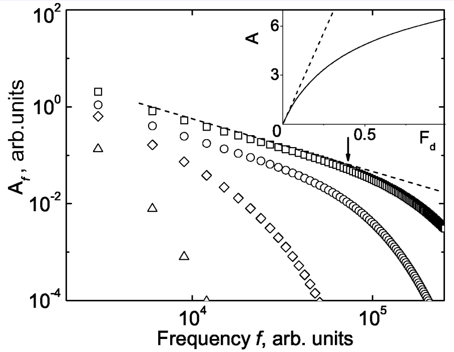

Very similar to experiments!

Viscous cut-off frequency

- Viscous cut-off frequencies as function of standing wave amplitude.
- Two temperatures: 1.77 K (lower) and 2.08 K (upper).
- Driving on 31st (filled symbols) or 32nd resonance.
- Dashed lines are by numerical calculation.

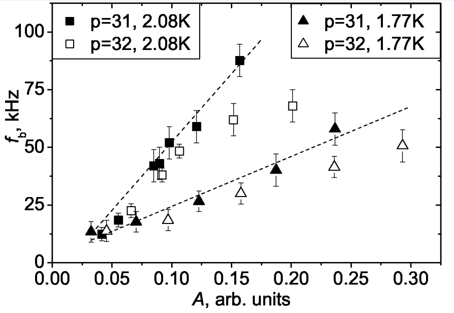

Evolution of power spectrum with drive frequency

- $T = 2.08$ K (negative nonlinearity), $W = 10\ \mathrm{mW\,cm^{-2}}$.
- Driving near 96th resonance: 9530.8 Hz (top); 9532.4 (middle); 9535.2 (bottom).
- Arrows –
  - Green: driving frequency
  - Blue: first harmonic
  - Red: region of subharmonic generation

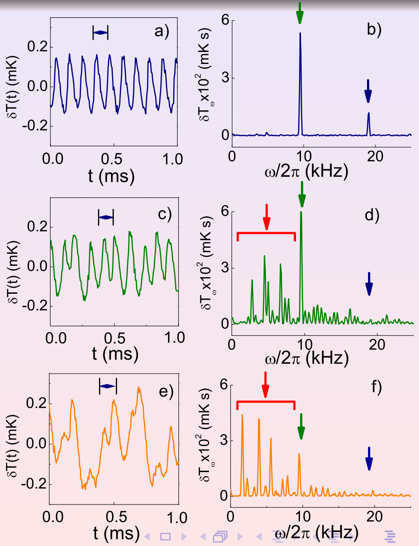

Evolution of power spectrum with drive amplitude

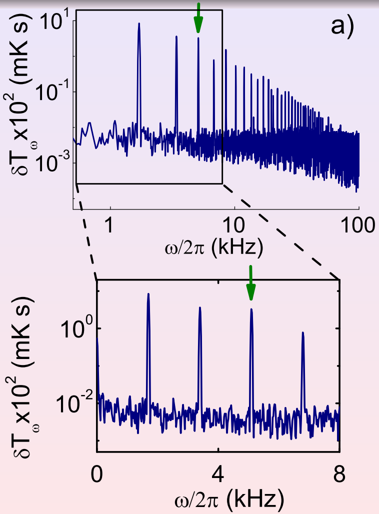

$W = 7$ mW cm^{-2}

Evolution of power spectrum with drive amplitude

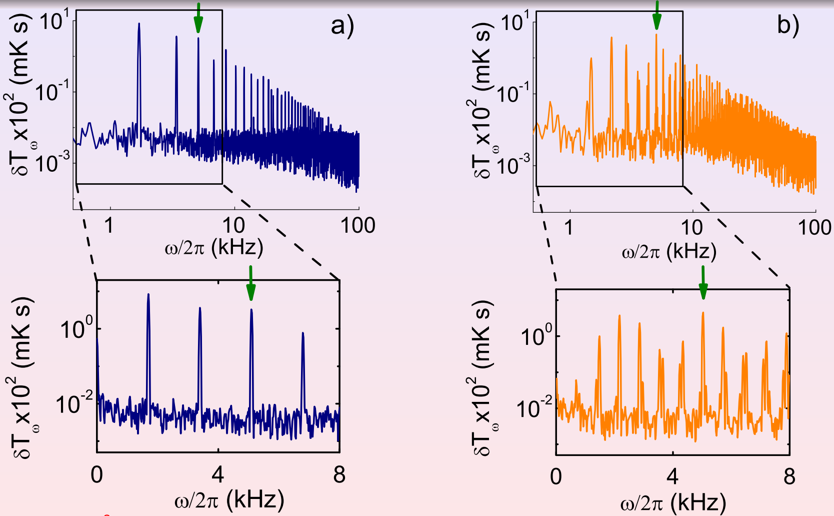

$W = 7$ mW cm^{-2}

$W = 20$ mW cm^{-2}

An inverse energy cascade

The experimental results show that, for the right conditions of wave amplitude and detuning –

- Wave energy flows to larger length scales.
- The onset of this inverse cascade is associated with an instability against formation of subharmonics.
- Onset is accompanied by a decrease in the energy of the regular cascade.
- Wave energy then gets dissipated at low frequencies – presumably due to the processes that reduce Q (normal fluid drag on the chamber walls?) at low frequencies.
- The onset of the inverse cascade sometimes involves hysteresis and metastability.

Conditions for onset instability and inverse cascade

Calculated heat flux W for onset of instability (full line) compared with experiment (data points) for different dimensionless detunings

$$\Delta = \frac{\omega_d - \omega_n}{\omega_n}$$

Bars indicate hysteretic width.

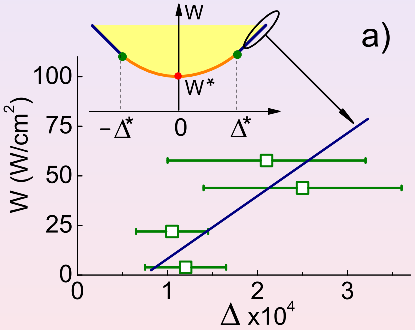

Conditions for onset instability and inverse cascade

Calculated heat flux *W* for onset of instability (full line) compared with experiment (data points) for different dimensionless detunings

$$\Delta = \frac{\omega_d - \omega_n}{\omega_n}$$

Bars indicate hysteretic width.

Bifurcation diagram (inset)

- Yellow ⇒ instability
- White ⇒ stability
- Orange line, soft instability
- Blue lines, hard instability
- Green points, critical points

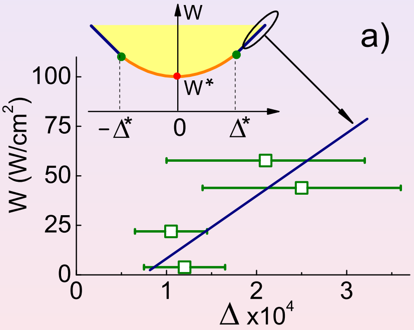

Power spectrum after development of instability

- Power spectrum of standing waves after onset of instability and inverse cascade.
- Green arrow: driving frequency ω_d.
- Inset: corresponding waveform, arrow shows driving period.

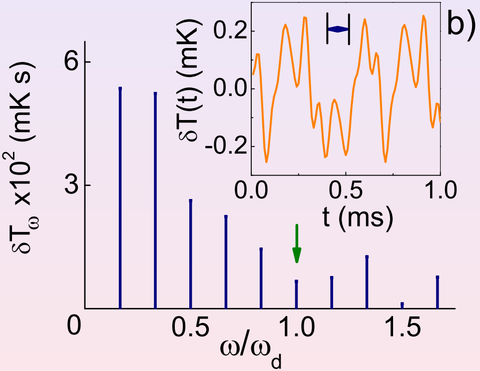

Energy can flow both ways

- Under the right conditions, energy in a turbulent acoustic system can flow towards the low frequency spectral domain.
- Inverse energy cascades are are also known in 2-D fluid flows.
- So the Kolmogorov picture, although correct for most of the time, is incomplete.

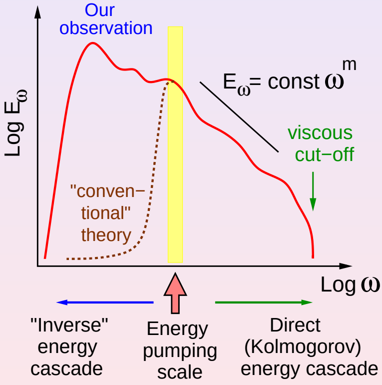

Effect of an additional low-frequency perturbation

- Driving on the 40$^{\text{th}}$ resonance, ω_{d1}.
- Note subharmonic at $\omega_{d1}/2$.

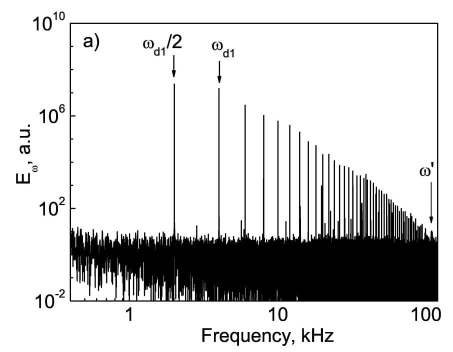

Effect of an additional low-frequency perturbation

- Driving on the 40th resonance, ω_{d1}.
- Note subharmonic at $\omega_{d1}/2$.
- Now add a small perturbation on the 9th resonance, ω_{d2}...

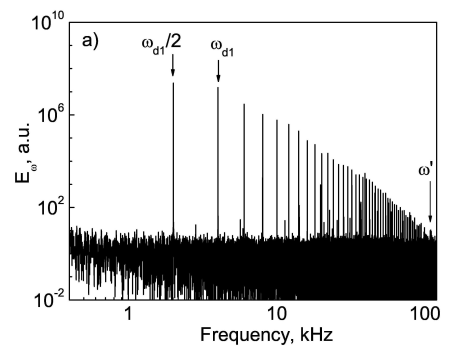

Effect of an additional low-frequency perturbation

- Driving on the 40th resonance, ω_{d1}.
- Note subharmonic at $\omega_{d1}/2$.
- Now add a small perturbation on the 9th resonance, ω_{d2}...
- Result is combination frequencies (cf. Stokes and anti-Stokes), and a dramatic fall at $\omega_{d1}/2$.
- Also, a reduction of the inertial interval (cf. H_2).

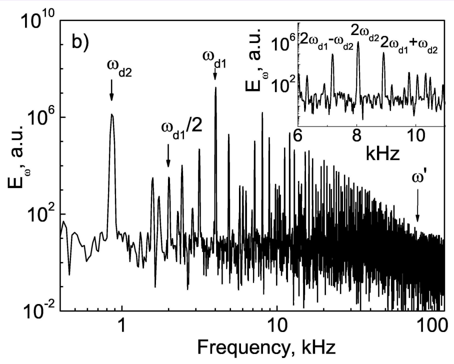

Outline

Time evolution of inverse cascade

A cornucopia of interesting transient effects, e.g.

- Driving near 51st resonance, starting at $t = 0$.
- Amplitudes of different low-frequency peaks plotted v. time t.
- Inverse cascade takes a long time to establish: 10–30 s (*cf* ~1 s for direct cascade).

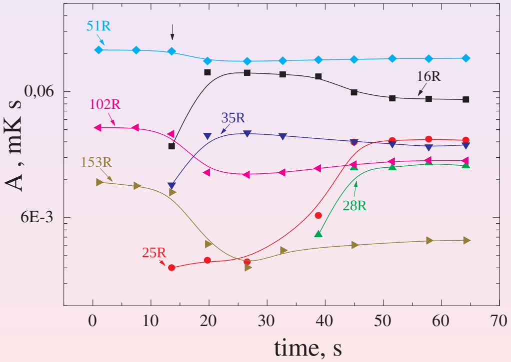

Evolution of acoustic turbulence

- Switch on drive at $t = 0$.
- Near 96$^{\text{th}}$ resonance, W=42 mW cm^{-2}, T=2.08 K.
- Direct cascade appears first.
- Inverse builds up slowly.
- Ultimately, nearly continuous.

Calculated evolution of inverse cascade

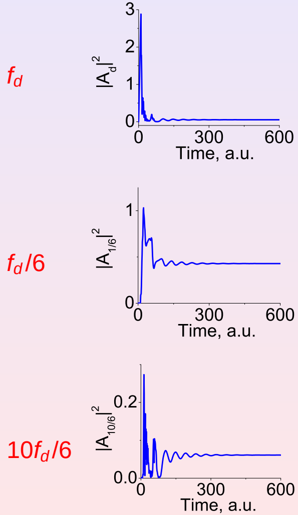

Calculated evolution of inverse cascade

f_d

$f_d/6$

$10f_d/6$

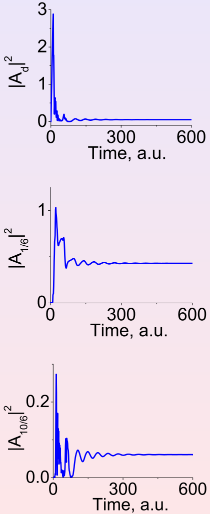

Steady state at $t \to \infty$

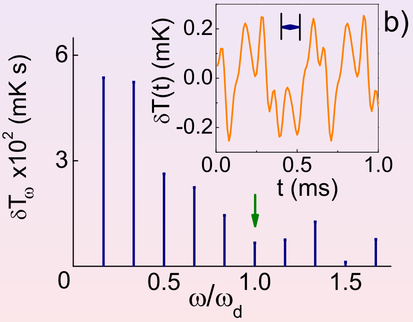

Steady state of inverse cascade

- Numerical calculation shows travelling waves within the resonator.

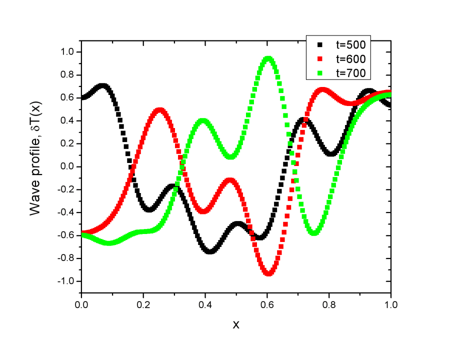

Outline

Origins of rogue waves?

- Dyachenko and Zakharov suggest "modulation instability of Stokes wave $\Rightarrow$ freak wave" (*JETP Lett*, 2005).
- First experimental observation of giant low-frequency waves, as predicted.
- NB oceanic surface involves 4-wave interactions, not 3-wave as here – but essential physics very similar.

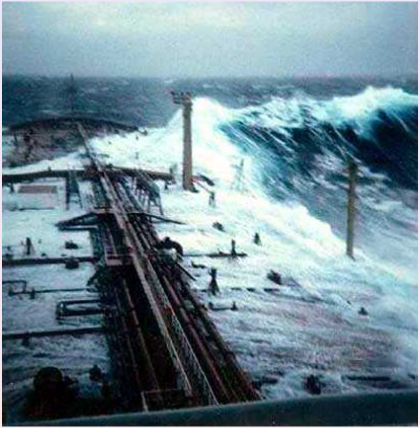

Other systems displaying wave turbulence

Features of wave turbulence observed and studied in He II are likely to appear for wave turbulence in other contexts, e.g. –

- Liquid surfaces.
- Bulk liquids and solids.
- Astrophysics.
- Plasma physics.

Most of these are far harder to control and study than He II – which provides a beautiful laboratory-scale model.

Outline

Conclusions I

- He II is uniquely suited to modelling nonlinear waves.
- The system of nonlinear second sound waves exhibits turbulence – with a Kolmogorov-like energy cascade towards high frequencies.
- Energy balance is nonlocal in K-space.
- The frequency scales of energy pumping and energy dissipation are widely separated.
- Addition of a second low frequency driving force leads to combination frequencies between it and the main drive.
- Amplitudes of second sound waves at high frequencies decrease when the extra driving is added – probably due to a redistribution of wave energy among newly excited states at low-frequencies.

Conclusions – II

- Under some conditions, an inverse cascade can exist, carrying energy towards frequencies lower than that at which it is pumped into the system – in addition to the conventional direct cascade.
- It leads to a substantial increase in wave amplitude at low frequency, corresponding to the formation of huge waves.
- It is apparently due to a modulation instability of the periodic wave – the same mechanism as that proposed to account for the creation of the rogue waves on the ocean.

Acknowledgements & selected references

We are grateful to EPSRC and the Russian Foundation for Basic Research for financial support.

1. G V Kolmakov, A A Levchenko, M Yu Brazhnikov, L P Mezhov-Deglin, A N Silchenko and P V E McClintock, "Quasi-adiabatic decay of capillary turbulence on the charged surface of liquid hydrogen", *Phys. Rev. Lett.* **93**, 074501 (2004).
2. G V Kolmakov, V B Efimov, A N Ganshin, P V E McClintock and L P Mezhov-Deglin, "Formation of a direct Kolmogorov-like cascade of second sound waves in He II", *Phys. Rev. Lett.* **97**, 155301 (2006).
3. A N Ganshin, V B Efimov, G V Kolmakov, L P Mezhov-Deglin and P V E McClintock, "Observation of giant low-frequency waves in developed acoustic turbulence in superfluid helium", *Phys. Rev. Lett* (in press).